IJE TRANSACTIONS A: Basics Vol. 31, No. 7, (July 2018) 1095-1102

International Journal of Engineering

Journal Homepage: www.ije.ir

Vibration Behavior of Nanocomposite Plate Reinforced by Pristine and Defective Graphene Sheets; an Analytical Approach

E. Allahyari, M. Asgari*

Faculty of Mechanical Engineering, K. N. Toosi University of Technology, Tehran, Iran

PAPER INFO

Paper history:
Received 05 December 2017
Received in revised form 14 January 2018
Accepted 09 March 2018

Keywords:
Nanocomposite
Graphene Sheets
Free Vibration
Eringen Nonlocal Theory
Vacancy Defect
Analytical Solution

ABSTRACT

Free vibration characteristics of polymer composite plates reinforced by graphene nanosheets employing the Eringen nonlocal elasticity theory were investigated. Theoretical formulations are derived based on Hamilton's principle implementing linear orthotropic constitutive equations of lamina while the behavior of nanostructure points affected by all other nonlocal points is also taken into account. For obtaining the mechanical properties, a new modified Halpin–Tsai model is employed. Governing equations are solved by developing an efficient analytical solution. The accuracy of the presented method is examined, by comparing the results with literature in which a good agreement is observed. Effects of different boundary conditions, volume fraction, graphene sheets orientation angle and Eringen nonlocal parameter on frequency of nanocomposite are analyzed. Effects of the presence of vacancy defects in the nanosheet on the behavior of reinforced composites were also studied. The results illustrate that by increasing the nonlocal parameter the natural frequency showed a decreasing trend while by increasing the graphene sheet's volume fraction, natural frequencies significantly increased. It could be concluded that the orientation angle variations in graphene sheets, did not play an important role on the natural frequency of nanocomposite as well as degradation of properties resulted in from vacancy defects.

***doi**: 10.5829/ije.2018.31.07a.13*

1. INTRODUCTION

Due to increasing the applications of nanocomposites reinforced with carbon based nanostructures including carbon nanofillers, need for accurate and effective analysis of behavior of such nanostructures has been increased in recent years. An efficient theory was introduced by Eringen [1]. Recently, some research works have been reported excellent solution methods using the nonlocal theory for nanostructure studies. For instance, Karličić et al. [2] used the nonlocal theory to examine the influence of in-plane magnetic field on the viscoelastic orthotropic multi-nanoplate system (VOMNPS) embedded in a viscoelastic medium. Pradhan and Phadikar [3] studied nonlocal elasticity theory for vibration of nanoplates. They employed both classical and FSDT of plates to analyze the vibration of single and double layer graphene sheets.

*Corresponding Author Email: *asgari@kntu.ac.ir* (M. Asgari)

On the other hand, because of magnificent mechanical, chemical, thermal and electrical material properties of nanosheets including graphene and also it's widely uses in several advanced industries; lots of esearchers have recently paid attention on nanosheets [4]. Shariyat et al. [5]employed a molecular mechanics approach to investigate the mechanical properties of nanosheet using a proper unit cell. Montazeri and Rafii-Tabar [6] employed different kinds of method to compute the elastic constants of a polymeric nanocomposite embedded with graphene sheets. Kitipornchai et al. [7] examined the vibration and the buckling of FGM beams reinforced by graphene platelets. Jalali et al. [8] examined the out-of-plane defects on vibrational analysis of single layered graphene sheets. Nazemnezhad [9] used nonlocal

Timoshenko beam model and molecular dynamics simulations to investigate the free vibration of cantilever multi-layer graphene nanoribbons. Arani et al. [10] used the third order shear deformation theory to study the

Please cite this article as: E. Allahyari, M. Asgari, Vibration Behavior of Nanocomposite Plate Reinforced by Pristine And Defective Graphene Sheets; an Analytical Approach, International Journal of Engineering (IJE), IJE TRANSACTIONS A: Basics Vol. 31, No. 7, (July 2018) 1095-1102

instability of axially moving single-layered graphene sheet. Accordingly, experimental and theoretical efforts have been carried out in order to study various kinds of effects on defected graphene sheets, in recent years. Allahyari and Fadaee [11] presented the vibration of circular double-layer graphene sheets with defect and surface effects. They employed an analytical investigation to compute the natural frequencies of nanoplate. So it is important to focus on vibrational behavior of nanocomposites which the graphene nanosheets are dispersed in them. For example, Yao et al. [12] studied about homogeneous dispersion of graphene nanosheets in epoxy. Ragavan et al. [13] developed Graphene magnetic nanocomposite as a nano-adsorbent. Gharib et al. [14] presented the vibrational behavior of polymeric nanocomposite. Mohammadimehr et al. [15] developed the free vibration of nanocomposite plate reinforced by functionally graded single-walled carbon nanotube embedded in viscoelastic foundation. While quite a few investigations on vibration characteristics of graphene reinforced polymer nanocomposite plates have been reported; there seems to be a void in studies concerning defected graphene nanosheets. Based on Eringen nonlocal elasticity theory, the constitutive equations by employing transformed orthotropic stiffness components were obtained. To estimate the mechanical properties of nanocomposite plate reinforced by graphene sheets, a new modified Halpin–Tsai model was used. In that a special procedure was employed to obtain the graphene efficiency parameters according to Halpin–Tsai model and the MD simulations.

2. THEORETICAL FORMULATION AND DEVELOPING ANALYTICAL SOLUTION

A rectangular nanocomposite reinforced by graphene sheet with length "a", width "b" and uniform thickness "h" is depicted in Figure 1. The origin of the considered coordinate system is placed at one end of the nanoplate on the mid-plane surface. The (x, y) are in the length and width directions of the nanocomposite, respectively. The z is placed in the direction of the outward normal to the mid-plane surface.

The differential constitutive equation of Eringen nonlocal theory [16] can be presented by the following form

$$(1-\mu\nabla^2)S^{nl}=S^{l} \tag{1}$$

where ∇^2 is the Laplacian operator, μ is the nonlocal parameter or small scale coefficient, S^{nl}, S^{l} are the nonlocal and the local stress tensor, respectively.

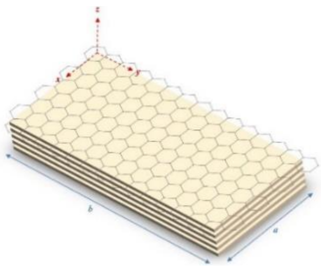

Figure 1. Schematic of a rectangular nanocomposite reinforced by pristine graphene sheet

According to the classical plate theory, displacement field for a rectangular single layer plate can be considered as follows:

$$\begin{aligned} u(x,y,z,t)&=u_0(x,y,t)-z(\partial w/\partial x)\\ v(x,y,z,t)&=v_0(x,y,t)-z(\partial w/\partial y)\\ w(x,y,z,t)&=w_0(x,y,t) \end{aligned} \tag{2}$$

Here (u_0,v_0,w_0) are called the midplane displacement and (u,v,w) are the displacements along x, y and z directions, respectively. Using the strain-displacement relations, the only nonzero strains are given by following experssions:

$$\begin{aligned} &\varepsilon_{xx}=(\frac{\partial u_0}{\partial x})-z(\frac{\partial^2 w}{\partial x^2}) \quad ,\varepsilon_{yy}=(\frac{\partial v_0}{\partial y})-z(\frac{\partial^2 w}{\partial y^2})\\ &\varepsilon_{xy}=\frac{1}{2}(\frac{\partial u_0}{\partial y}+\frac{\partial v_0}{\partial x}-2z\,\frac{\partial^2 w}{\partial x\,\partial y}) \end{aligned} \tag{3}$$

According to Eringen nonlocal theory and using orthotropic constitutive equations of lamina, it can be represented as follows:

$$(1-\mu\nabla^2)\begin{bmatrix} S_{xx}^{nl}\\ S_{yy}^{nl}\\ S_{xy}^{nl}\end{bmatrix}=\begin{bmatrix}\bar{T}_{11} & \bar{T}_{12} & \bar{T}_{16}\\ \bar{T}_{12} & \bar{T}_{22} & \bar{T}_{26}\\ \bar{T}_{16} & \bar{T}_{26} & \bar{T}_{66}\end{bmatrix}\begin{Bmatrix}\varepsilon_{xx}^{nl}\\ \varepsilon_{yy}^{nl}\\ \varepsilon_{xy}^{nl}\end{Bmatrix} \tag{4}$$

Here $\bar{T}_{ij}$ denote the transformed stiffness components and is defined as follows [17]:

$$\begin{aligned} \bar{T}_{11}&=(T_{11}c^4)+2(T_{12}+2T_{66})c^2s^2+T_{22}s^4\\ \bar{T}_{12}&=(T_{11}+T_{22}-4T_{66})c^2s^2+T_{12}(s^4+c^4)\\ \bar{T}_{22}&=(T_{11}s^4)+2(T_{12}+2T_{66})c^2s^2+(T_{22}c^4)\\ \bar{T}_{16}&=(T_{11}-T_{12}-2T_{66})c^3s+(T_{11}-T_{22}+2T_{66})s^3c\\ \bar{T}_{26}&=(T_{11}-T_{12}-2T_{66})cs^3+(T_{11}-T_{22}+2T_{66})sc^3\\ \bar{T}_{66}&=(T_{11}+T_{22}-2T_{12}-2T_{66})c^2s^2+T_{66}(s^4+c^4) \end{aligned} \tag{5}$$

in which $c=\cos(\theta)$, $s=\sin(\theta)$ and θ is the orientation angle between the global and local Cartesian coordinates. Also T_{ij} are the components of stiffness tensor in the following form:

$$T_{11} = \frac{E_1}{1-(\nu_{12}\nu_{21})}, T_{12} = \frac{\nu_{12}E_2}{1-(\nu_{12}\nu_{21})}, T_{22} = \frac{E_2}{1-(\nu_{12}\nu_{21})}$$
$$T_{66} = G_{12}, \nu_{21} = \frac{\nu_{12}E_2}{E_1} \tag{6}$$

It is assumed that the graphene sheets are uniformly distributed within the plate thickness. To obtain mechanical properties of nanocomposite plate, a new modified Halpin–Tsai model is employed [17]:

$$E_1 = (E^m\eta_1)\left(\frac{1+2(a_G/h_G)\lambda_{11}V^G}{(1-\lambda_{11}V^G)}\right), E_2 = (E^m\eta_2)\left(\frac{1+2(b_G/h_G)\lambda_{22}V^G}{(1-\lambda_{22}V^G)}\right)$$
$$G_{12} = (G^m\eta_3)\left(\frac{1}{1-\lambda_{12}V^G}\right), \nu_{12} = (V^G\nu_{12}^G) + (1-V^G)\nu^m \tag{7}$$
$$\rho = (V^G\rho^G) + (1-V^G)\rho^m$$

where, ac, bc and hc are the length, width and effective thickness of graphene sheet, respectively.

$$\lambda_{11} = \left(\frac{(E_1^G/E^m)-1}{(E_1^G/E^m)+2(a_G/h_G)}\right)$$
$$\lambda_{22} = \left(\frac{(E_2^G/E^m)-1}{(E_2^G/E^m)+2(b_G/h_G)}\right) \tag{8}$$
$$\lambda_{12} = \left(\frac{(G_{12}^G/G^m)-1}{(G_{12}^G/G^m)}\right)$$

where, superscripts G and m represent the graphene and matrix, respectively. E_1 and E_2 are the elasticity modulus in longitudinal and transverse directions, respectively. G_{12} is the shear modulus. V^G denotes the graphene sheet volume fraction and ν_{12}, ρ are Poisson's ratio and density, respectively . Also η_i (i = 1, 2, 3) are called graphene efficiency parameters [18] to consider small scale effect. Now by substituting Equatios (6), (7) and (8) into Equation (5), it can be concluded that

$$\bar{T}_{11} = 2\cos^2(\theta)\sin^2(\theta)[\chi\eta_3 + \zeta\eta_2(V^G\nu_{12}^G + (1-V^G)\nu^m)]$$
$$+\psi\eta_2\sin^4(\theta) + \psi\eta_1\cos^4(\theta)$$
$$\bar{T}_{12} = \cos^2(\theta)\sin^2(\theta)(-2\chi\eta_3 + \psi\eta_1) + \zeta\eta_2$$
$$+[\cos^4(\theta)+\sin^4(\theta)]\zeta\eta_2(V^G\nu_{12}^G + (1-V^G)\nu^m)$$
$$\bar{T}_{22} = 2\cos^2(\theta)\sin^2(\theta)[\chi\eta_3 + \zeta\eta_2(V^G\nu_{12}^G + (1-V^G)\nu^m)]$$
$$+\zeta\eta_1\sin^4(\theta) + \zeta\eta_2\cos^4(\theta)$$
$$\bar{T}_{16} = \cos(\theta)\sin^3(\theta)[\chi\eta_3 + \psi\eta_1 - \zeta\eta_2] \tag{9}$$
$$+\cos^3(\theta)\sin(\theta)[-\chi\eta_3 + \psi\eta_1 - \zeta\eta_2(V^G\nu_{12}^G + (1-V^G)\nu^m)]$$
$$\bar{T}_{26} = \cos^3(\theta)\sin(\theta)[\chi\eta_3 + \psi\eta_1 - \zeta\eta_2]$$
$$+\cos(\theta)\sin^3(\theta)[-\chi\eta_3 + \psi\eta_1 - \zeta\eta_2(V^G\nu_{12}^G + (1-V^G)\nu^m)]$$
$$\bar{T}_{66} = \chi\eta_3[\cos^2(\theta)\sin^2(\theta)]$$
$$+\cos^2(\theta)\sin^2(\theta)[\chi\eta_3 + \zeta\eta_2(V^G\nu_{12}^G + (1-V^G)\nu^m)]$$
$$+\zeta\eta_2 - \zeta\eta_2(V^G\nu_{12}^G + (1-V^G)\nu^m)$$

where,

$$\psi = E^m\left[1+\frac{2(-1+E_1^G/E^m)V^Ga_G}{(E_1^G/E^m+2a_G/h_G)h_G}\right]/\left(1-\frac{(-1+E_1^G/E^m)V^G}{(E_1^G/E^m+2a_G/h_G)}\right)$$
$$\left[1-\frac{\eta_2(V^G\nu_{12}^G+(1-V^G)\nu^m)^2\left(1-\frac{(-1+E_1^G/E^m)V^G}{(E_1^G/E^m+2a_G/h_G)}\right)\left(1+\frac{2(-1+E_2^G/E^m)V^Gb_G}{(E_2^G/E^m+2b_G/h_G)h_G}\right)}{\eta_1\left(1-\frac{(-1+E_2^G/E^m)V^G}{(E_2^G/E^m+2b_G/h_G)}\right)\left[1+\frac{2(-1+E_1^G/E^m)V^Ga_G}{(E_1^G/E^m+2a_G/h_G)h_G}\right]}\right]$$
$$\zeta = E^m(1+2(-1+E_2^G/E^m)V^Gb_G/(E_2^G/E^m+2b_G/h_G)h_G)/\left(1-\frac{(-1+E_2^G/E^m)V^G}{(E_2^G/E^m+2b_G/h_G)}\right) \tag{10}$$
$$\left[1-\frac{\eta_2(V^G\nu_{12}^G+(1-V^G)\nu^m)^2\left(1-\frac{(-1+E_1^G/E^m)V^G}{E_1^G/E^m+2a_G/h_G}\right)\left(1+\frac{2(-1+E_2^G/E^m)V^Gb_G}{(E_2^G/E^m+2b_G/h_G)h_G}\right)}{\eta_1\left(1-\frac{(-1+E_2^G/E^m)V^G}{(E_2^G/E^m+2b_G/h_G)}\right)\left(1+\frac{2(-1+E_1^G/E^m)V^Ga_G}{(E_1^G/E^m+2a_G/h_G)h_G}\right)}\right]$$
$$\chi = \frac{E^m}{(1+\nu^m)\left(1-\frac{E^mV^G\left(-1+\frac{2G_{12}^G(1+\nu^m)}{E^m}\right)}{2G_{12}^G(1+\nu^m)}\right)}$$

The resultants force and moment components per unit length based on nonlocal stress tensors are defined as follows:

$$N_{xx} = \int_{-h/2}^{h/2} S_{xx}^{nl}dz, \quad M_{xx} = \int_{-h/2}^{h/2} S_{xx}^{nl}zdz$$
$$N_{yy} = \int_{-h/2}^{h/2} S_{yy}^{nl}dz, \quad M_{yy} = \int_{-h/2}^{h/2} S_{yy}^{nl}zdz \tag{11}$$
$$N_{xy} = \int_{-h/2}^{h/2} S_{xy}^{nl}dz, \quad M_{xy} = \int_{-h/2}^{h/2} S_{xy}^{nl}zdz$$

The equation of motion can be derived using Hamilton's principle as follows:

$$\int_0^T(\delta U + \delta V - \delta K)\,dt = 0 \tag{12}$$

Here *U* is the strain energy, *V* is the virtual work done by external applied forces and *K* is the kinetic energy. The variation of kinetic energy is obtained as follows:

$$\delta K = \frac{1}{2}\rho\int_V \delta(\dot{u}^2+\dot{v}^2+\dot{w}^2)dV$$
$$= \rho\int_V \delta(\dot{u}\delta\dot{u}+\dot{v}\delta\dot{v}+\dot{w}\delta\dot{w})dV$$
$$= \int_A [(I_0\dot{u} - I_1\frac{\partial\dot{w}}{\partial x})\delta\dot{u} + (-I_1\dot{u} - I_2\frac{\partial\dot{w}}{\partial x})\frac{\partial\delta\dot{w}}{\partial x} \tag{13}$$
$$+(I_0\dot{v} - I_1\frac{\partial\dot{w}}{\partial y})\delta\dot{v} + (-I_1\dot{v} + I_2\frac{\partial\dot{w}}{\partial y})\frac{\partial\delta\dot{w}}{\partial y} + (I_0\dot{w})\delta\dot{w}]dA$$

For the virtual strain energy, it can be mentioned that

$$\delta U = \int_A\int_{-h/2}^{h/2}(S_{xx}^{nl}\delta\varepsilon_{xx} + S_{yy}^{nl}\delta\varepsilon_{yy} + 2S_{xy}^{nl}\delta\varepsilon_{xy})\,dzdA$$
$$= \int_A [N_{xx}^{nl}\delta\varepsilon_{xx}^0 - M_{xx}^{nl}\frac{\partial^2\delta w}{\partial x^2} + N_{yy}^{nl}\delta\varepsilon_{yy}^0 \tag{14}$$
$$-M_{yy}^{nl}\frac{\partial^2\delta w}{\partial y^2} + 2N_{xy}^{nl}\delta\varepsilon_{xy}^0 - 2M_{xy}^{nl}\frac{\partial^2\delta w}{\partial x\partial y}]dA$$

The mass moments of inertia are defined as follows:

$$I_i = \int_A \rho z^i dA \,, i = 0,1,2 \tag{15}$$

Using integration by parts and vanishing some terms, finally the motion equations can be expressed as follows [3]:

$$\begin{aligned}
&(\frac{\partial N_{xx}}{\partial x} + \frac{\partial N_{yy}}{\partial y}) = \rho h \frac{\partial^2 u}{\partial t^2}, (\frac{\partial N_{xy}}{\partial x} + \frac{\partial N_{yy}}{\partial y}) = \rho h \frac{\partial^2 v}{\partial t^2} && \text{(a)}\\
&(\frac{\partial^2 M_{xx}}{\partial x^2} + 2\frac{\partial^2 M_{xy}}{\partial x \partial y} + \frac{\partial^2 M_{yy}}{\partial y^2}) + \frac{\partial}{\partial x}(N_{xx}\frac{\partial w}{\partial x} + N_{xy}\frac{\partial w}{\partial y}) && \text{(b)}\\
&+\frac{\partial}{\partial y}(N_{xy}\frac{\partial w}{\partial x} + N_{yy}\frac{\partial w}{\partial y}) = \rho h \frac{\partial^2 w}{\partial t^2} && \text{(c)}
\end{aligned} \tag{16}$$

The solution of Equation (16c) for fully simply supported rectangular plates (SSSS) can be obtained using Navier's method [19]. In this approach, the displacement is expanded in trigonometric series as

$$w(x,y,t) = \sum_{n=1}^{\infty}\sum_{m=1}^{\infty} W_{mn} \sin(\frac{m\pi x}{a})\sin(\frac{n\pi y}{b}) e^{i\omega t} \tag{17}$$

In which, m and n are mode numbers. Substituting Equation (17) into Equation (16c), the final equation for SSSS condition can be concluded

$$\begin{aligned}
&a^4h^2n^4\pi^4[2\cos^2(\theta)\sin^2(\theta)[\chi\eta_3+\zeta\eta_2(V^G v_{12}^G+(1-V^G)v^m)]\\
&+\zeta\eta_1\sin^4(\theta)+\zeta\eta_2\cos^4(\theta)]+2a^2b^2n^2\pi^2[(h^2m^2\pi^2(\cos^2(\theta)\sin^2(\theta)[-2\chi\eta_3+\psi\eta_1]\\
&+\zeta\eta_2+[\cos^4(\theta)+\sin^4(\theta)]\zeta\eta_2(V^G v_{12}^G+(1-V^G)v^m))+2[\chi\eta_3[\cos^2(\theta)\sin^2(\theta)]\\
&+\cos^2(\theta)\sin^2(\theta)[\chi\eta_3+\zeta\eta_2(V^G v_{12}^G+(1-V^G)v^m)]+\zeta\eta_2-\zeta\eta_2(V^G v_{12}^G+(1-V^G)v^m)]\\
&-6a^2\mu\rho\omega^2]+b^4[h^2m^4\pi^4(2\cos^2(\theta)\sin^2(\theta)[\chi\eta_3+\zeta\eta_2(V^G v_{12}^G+(1-V^G)v^m)]\\
&+\psi\eta_2\sin^4(\theta)+\psi\eta_1\cos^4(\theta)]-12a^2(a^2+m^2\pi^2\mu)\rho\omega^2]=0
\end{aligned} \tag{18}$$

Finally, it can be observed that the Equation (18) is in terms of ω, so the natural frequencies can be obtained. The Lévy method can be used to determine natural frequencies of rectangular plates for which two opposite edges are simply supported and the other two edges have any combination of Clamped (C), simply supported (S), and Free (F) boundary conditions. The solution is in the form of a single Fourier series as follow:

$$w(x,y,t) = W(y)\sin(\frac{m\pi x}{a}) e^{i\omega t} \tag{19}$$

that satisfies the simply supported boundary conditions as follows:

$$w = 0, M_{xx} = -(D_{11}\frac{\partial^2 w}{\partial x^2} + D_{12}\frac{\partial^2 w}{\partial y^2}) = 0 \tag{20}$$

Substituting Equation (19) into Equation (16c), it can be obtained:

$$\begin{aligned}
&[h^2m^4\pi^4(2\cos^2(\theta)\sin^2(\theta)[\chi\eta_3+\zeta\eta_2(V^G v_{12}^G+(1-V^G)v^m)]\\
&+\psi\eta_2\sin^4(\theta)+\psi\eta_1\cos^4(\theta))-12a^2(a^2+m^2\pi^2\mu)\rho\omega^2]W(y)\\
&+a^2(-2(h^2m^2\pi^2(\cos^2(\theta)\sin^2(\theta)[-2\chi\eta_3+\psi\eta_1]+\zeta\eta_2)\\
&+[\cos^4(\theta)+\sin^4(\theta)]\zeta\eta_2(V^G v_{12}^G+(1-V^G)v^m))\\
&+2(\chi\eta_3[\cos^2(\theta)\sin^2(\theta)]+\cos^2(\theta)\sin^2(\theta)\\
&[h^2m^4\pi^4(2\cos^2(\theta)\sin^2(\theta)[\chi\eta_3+\zeta\eta_2(V^G v_{12}^G+(1-V^G)v^m)]\\
&+\zeta\eta_2-\zeta\eta_2(V^G v_{12}^G+(1-V^G)v^m))]-6a^2\mu\rho\omega^2]W''(y)\\
&+a^2h^2[2\cos^2(\theta)\sin^2(\theta)(h^2m^4\pi^4(2\cos^2(\theta)\sin^2(\theta)\\
&[\chi\eta_3+\zeta\eta_2(V^G v_{12}^G+(1-V^G)v^m)]+\zeta\eta_1\sin^4(\theta)+\zeta\eta_2\cos^4(\theta))W^{(4)}(y))]=0
\end{aligned} \tag{21}$$

The ordinary differential equation (21) obtained in the Lévy method can be solved for the natural frequencies and mode shapes analytically. The form of the solution depends on the nature of the roots δ of the characteristics equation is given by following experssions:

$$\begin{aligned}
&h^2m^4\pi^4[2\cos^2(\theta)\sin^2(\theta)[\chi\eta_3+\zeta\eta_2(V^G v_{12}^G+(1-V^G)v^m)]\\
&+\psi\eta_2\sin^4(\theta)+\psi\eta_1\cos^4(\theta)]-12a^2(a^2+m^2\pi^2\mu)\rho\omega^2\\
&-2a^2(h^2m^2\pi^2(\cos^2(\theta)\sin^2(\theta)(-2\chi\eta_3+\psi\eta_1)+\zeta\eta_2\theta\\
&+[\cos^4(\theta)+\sin^4()]\zeta\eta_2(V^G v_{12}^G+(1-V^G)v^m))\\
&+2(\chi\eta_3[\cos^2(\theta)\sin^2(\theta)]+\cos^2(\theta)\sin^2(\theta)\\
&[\chi\eta_3+\zeta\eta_2(V^G v_{12}^G+(1-V^G)v^m)]+\zeta\eta_2\\
&-\zeta\eta_2(V^G v_{12}^G+(1-V^G)v^m))]-6a^2\mu\rho\omega^2]\,\delta^2\\
&+a^2h^2[2\cos^2(\theta)\sin^2(\theta)[\chi\eta_3+\zeta\eta_2(V^G v_{12}^G+(1-V^G)v^m)]\\
&+\zeta\eta_1\sin^4(\theta)+\zeta\eta_2\cos^4(\theta)]\,\delta^4=0
\end{aligned} \tag{22}$$

The general solution of Equation (22) is given by

$$\begin{aligned}
&W(y) = \bar{A}\cosh(R_1 y) + \bar{B}\sinh(R_1 y)\\
&+\bar{C}\cos(R_2 y) + \bar{D}\sin(R_2 y)
\end{aligned} \tag{23}$$

Also, $\bar{A}$, $\bar{B}$, $\bar{C}$ and $\bar{D}$ are integration constants, which are determined using the boundary conditions. However, we do not actually determine these constants. Instead, the values of ω are determined by setting the determinant of the coefficient matrix $\bar{A}$, $\bar{B}$, $\bar{C}$ and $\bar{D}$ to zero. For SSSF boundary condition, it can be stated follows:

$$\begin{aligned}
&w = 0, M_{yy} = -(D_{12}\frac{\partial^2 w}{\partial x^2} + D_{22}\frac{\partial^2 w}{\partial y^2}) = 0 \;\; on \;\; y = 0\\
&M_{yy} = 0, V_y = -(\bar{D}_{12}\frac{\partial^3 w}{\partial x^2 \partial y} + D_{22}\frac{\partial^3 w}{\partial y^3}) = 0 \;\; on \;\; y = b
\end{aligned} \tag{24}$$

For the solution of Equation (23) in this case, the boundary conditions in Equation (24) and yield $A = C = 0$. Setting the determinant of the coefficient matrix to zero, we obtain the following characteristic equation for the natural vibration of SSSF plates. For SSCC boundary condition, it can be mentioned below:

$$w = 0, (\frac{\partial w}{\partial y}) = 0 \quad on \quad y = 0, b \tag{25}$$

Substitution of Equation (23) into Equation (25) yields the following characteristic equation:

$$2[1 - \cosh(R_1 b)\cos(R_2 b)] + (R_1 / R_2 - R_2 / R_1) \sinh(R_1 b)\sin(R_1 b) = 0 \tag{26}$$

3. RESULTS AND DISCUSSIONS

In this part, in order to show the convergence and accuracy of the presented method, a comparison study for variation of natural frequencies ratio with length of a square nanoplate for various nonlocal parameter is illustrated in Figure 2. The results obtained from the developed analytical method has been compared with results of Pradhan and Phadikar [3]. The mechanical properties are supposed to be the same as, elastic modulus, $E = 1.02\,\text{Tpa}$, thickness of the graphene plate, $h = 0.34\,\text{nm}$, density, $\rho = 2750\,\text{kg/m}^3$ and the Poisson's ratio, $\nu = 0.3$. Results depicted in Figure 2 shows that an exceptional convergence and agreement with different value of nonlocal parameter is obtained.

Based on this fact, in order to examine the accuracy of the developed method, another comparison study for the effect of volume fraction on the dimensionless fundamental frequency of an CNT reinforce nanocomposite plate is summarized in Table 1. It is obvious that the present results have good agreement with literature. According to Table 2, it can be observed that as the nonlocal parameter increases, the stiffness of nanocomposite decreases thus the natural fundamental frequencies decrease. It can be clearly seen that the frequency is significantly increased by increasing a small amount of graphene nanosheets into the polymer matrix. Table 3 reports the natural fundamental frequencies of nanocomposites reinforced with graphene sheets for various orientation angles and volume fractions with SSSF boundary condition. Figure 3 shows that as the nonlocal parameters increases the natural frequencies decrease.

Schematic representation of a defect-free graphene sheet and with the presence of vacancy defects are shown in Figure 4. Based on the results obtained through molecular dynamics simulations reported by Hao et al. [20], dependency of Young's modulus of a monolayer graphene sheet with monatomic vacancies to the concentration of monatomic vacancies could be realized. For the mechanical properties, it can be seen that Young's moduli of defected graphene sheets feature a linear dependence on the defect concentration.

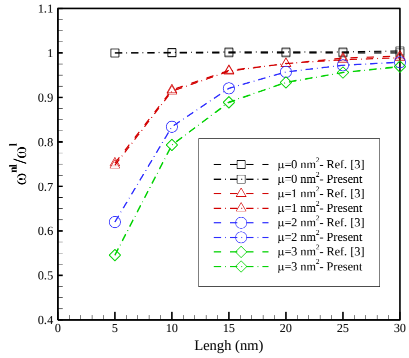

Figure 2. Natural frequencies ratio with the length of a square nanoplate for various nonlocal parameter obtained by numerical and analytical solutions

TABLE 1. Effect of volume fraction on the nondimensional fundamental frequency of CNT reinforced composite square plate for SSSS condition

V^{CNT}	Modes (m,n)	Zhu et al. [21]	Alibeigloo [22]	Wu & Li [23]	Present
0.11	(1,1)	19.223	19.168	19.155	19.486
	(1,2)	23.408	23.270	23.273	23.387
	(1,3)	34.669	34.054	34.038	34.049
0.14	(1,1)	21.354	21.328	21.317	21.807
	(1,2)	25.295	25.199	25.188	25.466
	(1,3)	36.267	35.679	35.667	35.808
0.17	(1,1)	23.679	23.622	23.607	23.994
	(1,2)	28.987	28.825	28.810	28.927
	(1,3)	43.165	42.386	42.367	42.357

TABLE 2. Natural frequencies (GHz) of nanocomposite plate for SSSS condition

$\mu(nm^2)$	V^G	Mode numbers (m,n)			
		(1,1)	(1,2)	(2,1)	(2,2)
0	0.03	158.491	398.644	401.822	633.965
	0.07	222.219	561.756	564.536	888.876
	0.11	239.861	599.105	603.165	959.454
1	0.03	154.720	376.118	379.116	579.358
	0.07	216.931	530.013	532.636	812.312
	0.11	234.155	565.251	569.082	876.811
2	0.03	151.205	357.024	359.870	536.799
	0.07	212.003	503.106	505.596	752.641
	0.11	228.836	536.556	540.192	812.401
3	0.03	147.920	340.571	343.285	502.423
	0.07	207.397	479.921	482.296	704.443
	0.11	223.846	511.829	515.298	760.376

TABLE 3. Natural frequencies (GHz) of nanocomposite plate for SSSF condition

$\mu(nm^2)$	V^G	$\hat{\theta}$			
		0	30	60	90
0	0.03	158.491	398.644	401.822	633.965
	0.07	222.219	561.756	564.536	888.876
	0.11	239.861	599.105	603.165	959.454
1	0.03	154.720	376.118	379.116	579.358
	0.07	216.931	530.013	532.636	812.312
	0.11	234.155	565.251	569.082	876.811
2	0.03	151.205	357.024	359.870	536.799
	0.07	212.003	503.106	505.596	752.641
	0.11	228.836	536.556	540.192	812.401
3	0.03	147.920	340.571	343.285	502.423
	0.07	207.397	479.921	482.296	704.443
	0.11	223.846	511.829	515.298	760.376

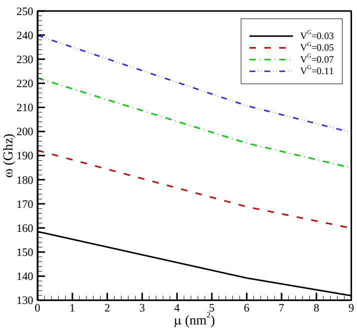

Figure 3. Natural frequencies of nanocomposite with pristine graphene sheets and orientation angle $\hat{\theta}=0^\circ$ for various nonlocal parameter, volume fractions and SSSS boundary condition

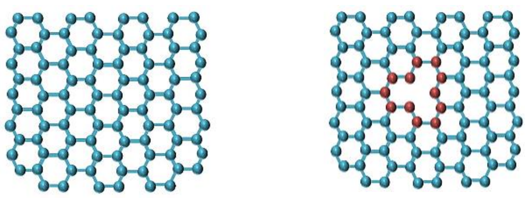

(a) (b)

Figure 4. Schematic representation of a) defect-free pristine graphene sheet b) presence of vacancy defect

Young's modulus of a defect-free graphene sheet is 1.1 TPa when a thickness of 3.2 nm is used. The curve can be fitted into a linear function for monatomic vacancies as $E^d = 1.8\times10^{12}(0.994-0.027f_v)$, which can be explained as that it contains two heptagons and two pentagons, which preserve interatomic sp^2 bonding, while monatomic vacancy breaks the integrity of pristine sheet that results in a higher formation energy in comparison with the nucleation energy for Stone-Wales dislocation. A linear fitting for the Stone-Wales dislocations fails here as is hard to define the concentration. Figure 5 shows the MD simulation results as well as a fitted liner curve.

Figure 6 shows the effects of nonlocal parameter versus the vacancy concentration of defected graphene sheets on natural frequencies of nanocomposite. The vacancy concentration is considered between 0-4% while the Eringen nonlocal parameter is taken 0-9 nm^2.

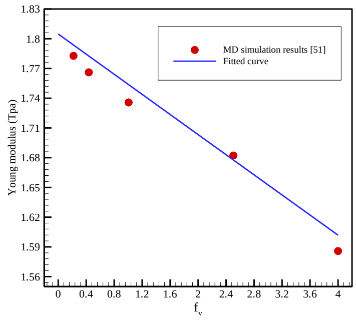

Figure 5. Young's modulus of defective graphene sheet versus concentration of monovacancy defect percent

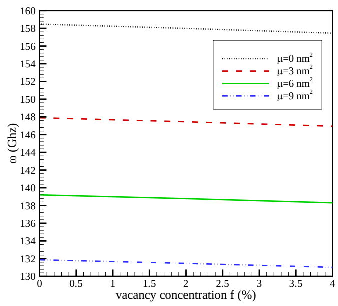

Figure 6. Effects of vacancy concentration in conjuring with the nonlocal parameter on natural frequencies of nanocomposite reinforced with defected graphene sheets for SSSS boundary condition**.**

4. CONCLUSION

In this work, an analytical investigation to examine the free vibration of nanocomposite reinforced by graphene sheets employing Eringen nonlocal elasticity theory was carried out. An effective analytical solution is developed for solving the complicated governing equations which is much more efficient in comparison to common numerical solutions. The accuracy of the presented method is examined, by comparing the results with literature in which a good agreement was observed. To show the novelty of the presented approach Eringen nonlocal theory as well as various orientation angles of defected and pristine graphene sheet reinforcement were considered together and solved base on an analytical method. It is also suggested that nonlocal parameter and volume fraction have a specific effect on natural frequencies, while various orientation angles of graphene sheets in nanocomposites have a slight effect on natural frequencies. By increasing the graphene sheets volume fraction, nanocomposite gets stiffer and the frequencies increase significantly, while as the nonlocal parameter decreases the nanocomposite frequencies increase.

5. REFERENCES

1. Eringen, A.C., "Nonlocal continuum field theories, Springer Science & Business Media, (2002).
2. Karličić, D., Kozić, P., Adhikari, S., Cajić, M., Murmu, T. and Lazarević, M., " Nonlocal mass-nanosensor model based on the damped vibration of single-layer graphene sheet influenced by in-plane magnetic field ", ***International Journal of Mechanical Sciences***, Vol. 96, (2015), 132-142.
3. Pradhan, S. and Phadikar, J., "Nonlocal elasticity theory for vibration of nanoplates", ***Journal of Sound and Vibration***, Vol. 325, No. 1-2, (2009), 206-223.
4. Hashemi, S.H. and Khaniki, H.B., "Analytical solution for free vibration of a variable cross-section nonlocal nanobeam", ***International Journal of Engineering-Transactions B: Applications***, Vol. 29, No. 5, (2016), 688-696.
5. Shariyat, M., Sarvi, Z. and Asgari, M., "A unit-cell-based three-dimensional molecular mechanics analysis for buckling load, effective elasticity and poisson's ratio determination of the nanosheets", ***Molecular Simulation***, Vol. 42, No. 5, (2016), 353-369.
6. Montazeri, A. and Rafii-Tabar, H., "Multiscale modeling of graphene-and nanotube-based reinforced polymer nanocomposites", ***Physics Letters A***, Vol. 375, No. 45, (2011), 4034-4040.
7. Kitipornchai, S., Chen, D. and Yang, J., "Free vibration and elastic buckling of functionally graded porous beams reinforced by graphene platelets", ***Materials & Design***, Vol. 116, (2017), 656-665.
8. Jalali, S., Jomehzadeh, E. and Pugno, N., "Influence of out-of-plane defects on vibration analysis of graphene: Molecular dynamics and non-local elasticity approaches", ***Superlattices and Microstructures***, Vol. 91, (2016), 331-344.
9. Nazemnezhad, R., "Nonlocal timoshenko beam model for considering shear effect of van der waals interactions on free vibration of multilayer graphene nanoribbons", ***Composite Structures***, Vol. 133, (2015), 522-528.
10. Arani, A.G., Haghparast, E. and Zarei, H.B., "Nonlocal vibration of axially moving graphene sheet resting on orthotropic visco-pasternak foundation under longitudinal magnetic field", ***Physica B: Condensed Matter***, Vol. 495, (2016), 35-49.
11. Allahyari, E. and Fadaee, M., "Analytical investigation on free vibration of circular double-layer graphene sheets including geometrical defect and surface effects", ***Composites Part B: Engineering***, Vol. 85, (2016), 259-267.
12. Yao, H., Hawkins, S.A. and Sue, H.-J., "Preparation of epoxy nanocomposites containing well-dispersed graphene nanosheets", ***Composites Science and Technology***, Vol. 146, (2017), 161-168.
13. Ragavan, K. and Rastogi, N.K., "Β-cyclodextrin capped graphene-magnetite nanocomposite for selective adsorption of bisphenol-a", ***Carbohydrate polymers***, Vol. 168, (2017), 129-137.
14. Gharib, A., Karimi, M.S. and Arani, A.G., "Vibration analysis of the embedded piezoelectric polymeric nano-composite panels in the elastic substrate", ***Composites Part B: Engineering***, Vol. 101, No., (2016), 64-76.
15. Mohammadimehr, M., Navi, B.R. and Arani, A.G., "Free vibration of viscoelastic double-bonded polymeric nanocomposite plates reinforced by fg-swcnts using msgt, sinusoidal shear deformation theory and meshless method", ***Composite Structures***, Vol. 131, No., (2015), 654-671.
16. Eringen, A.C., "On differential equations of nonlocal elasticity and solutions of screw dislocation and surface waves", ***Journal of applied physics***, Vol. 54, No. 9, (1983), 4703-4710.
17. Affdl, J.H. and Kardos, J., "The halpin-tsai equations: A review", ***Polymer Engineering & Science***, Vol. 16, No. 5, (1976), 344-352.
18. Shen, H.-S., "Nonlinear bending of functionally graded carbon nanotube-reinforced composite plates in thermal environments", ***Composite Structures***, Vol. 91, No. 1, (2009), 9-19.
19. Reddy, J.N., "Theory and analysis of elastic plates and shells, CRC press, (2006).
20. Hao, F., Fang, D. and Xu, Z., "Mechanical and thermal transport properties of graphene with defects", ***Applied physics letters***, Vol. 99, No. 4, (2011), 041901.
21. Zhu, P., Lei, Z. and Liew, K.M., "Static and free vibration analyses of carbon nanotube-reinforced composite plates using finite element method with first order shear deformation plate theory", ***Composite Structures***, Vol. 94, No. 4, (2012), 1450-1460.
22. Alibeigloo, A. and Emtehani, A., "Static and free vibration analyses of carbon nanotube-reinforced composite plate using differential quadrature method", ***Meccanica***, Vol. 50, No. 1, (2015), 61-76.
23. Wu, C.-P. and Li, H.-Y., "Three-dimensional free vibration analysis of functionally graded carbon nanotube-reinforced composite plates with various boundary conditions", ***Journal of Vibration and Control***, Vol. 22, No. 1, (2016), 89-107.

Vibration Behavior of Nanocomposite Plate Reinforced by Pristine and Defective Graphene Sheets; an Analytical Approach

E. Allahyari, M. Asgari

Faculty of Mechanical Engineering, K. N. Toosi University of Technology, Tehran, Iran

PAPER INFO

Paper history:
Received 05 December 2017
Received in revised form 14 January 2018
Accepted 09 March 2018

Keywords:
Nanocomposite
Graphene Sheets
Free Vibration
Eringen Nonlocal Theory
Vacancy Defect
Analytical Solution

چکیده

ارتعاش آزاد ورق‌های کامپوزیت پلیمری که با نانوورق‌های گرافن تجهیز شده‌اند با استفاده از تئوری الاستیسیته غیرمحلی ارینگن مورد بررسی قرار گرفته‌اند. روابط تئوری با بکارگیری اصل همیلتون و معادلات خطی و ساختاری چندلایه ارتوتروپیک که نیز در آن رفتار نقاطی از نانوسازه تحت تاثیر دیگر نقاط غیرمحلی می‌باشد استخراج شده است. به‌منظور به دست آوردن خواص مکانیکی، فرم ارتقاء یافته هالفین-تسای بکار گرفته شده است. معادلات پایه با استفاده از یک روش تحلیلی به دست آمده‌اند. دقت روش ارائه شده با مقایسه نتایج آن با دیگر مقالات بررسی شده است که تطابق خوبی مشاهده شده است. اثرات شرایط مرزی مختلف، درصد حجمی، زاویه جهت‌گیری ورق‌های گرافن و پارامتر غیرمحلی ارینگن بر روی فرکانس نانوکامپوزیت مورد بررسی قرار گرفته‌اند. اثرات وجود عیوب شبکه در نانوورق بر روی رفتار کامپوزیت‌های تقویت شده نیز مورد بررسی قرار گرفته‌اند. نتایج نشان می‌دهد که با افزایش پارامتر غیرمحلی فرکانس طبیعی تمایل به نشان دادن رفتاری نزولی دارد درحالیکه با افزایش درصد حجمی نانو گرافن، فرکانس‌های طبیعی به طور محسوسی افزایش می‌یابند. می‌توان نتیجه گرفت که زوایای مختلف جهت‌گیری ورق‌های گرافن همچنین افت خواص ایجاد شده به واسطه عیوب شبکه، نقش مهمی در فرکانس طبیعی نانوکامپوزیت نخواهند داشت.

***doi**: 10.5829/ije.2018.31.07a.13*